ELECTROMAGNETIC FORCING OF A SEAWATER FLOW : EXPERIMENTAL AND NUMERICAL STUDIES

François Bouillon, Claudio Lindquist, Sedat Tardu & Jean-Paul Thibault
LEGI – Laboratoire des Ecoulements Géophysiques et Industriels
BP 53, 38041 38041 GRENOBLE Cedex, France
francois.bouillon@hmg.inpg.fr claudio.lindquist@hmg.inpg.fr
sedat.tardu@hmg.inpg.fr jean-paul.thibault@hmg.inpg.fr

ABSTRACT

Seawater Electromagnetic Flow Control (EMFC) is a research field with promising naval applications. In this context, EMFC may be employed to reduce skin friction and turbulence intensity, and to prevent boundary layer separation. In fact, experimental results presented in the literature have shown significant drag and turbulent intensity reductions of a turbulent flow by using an array of electromagnetic (EM) actuators (Nosenchuck & Brown 1993, Bandyopadhay 1998). The present work aims to give a better understanding of the possible mechanisms involved in EM forcing of a seawater flow. Firstly, an experiment about EM forcing of an hairpin vortex street is described, and secondly a numerical simulation (DNS) of various forcing protocols is presented. Both aim at a better understanding of the physical mechanisms involved in EMFC.

INTRODUCTION

The principle of Electromagnetic Flow Control (EMFC) is based on the direct injection of local body forces into the flow close to the wall. The EM force field **F**, also know as Lorentz force, is induced by the cross product of the electric current density **j** and the magnetic induction field **B**, imposed by wall-flushed electrodes and permanent magnets, respectively. Figure 1 illustrates an EM actuator, called normal EM actuator due to the resulting force that is mostly perpendicular to the wall.

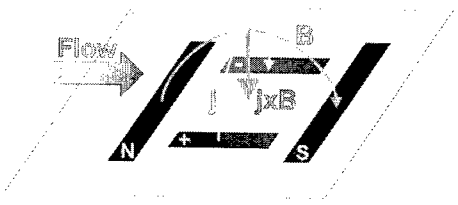

Figure 1 : Schematic normal EM actuator.

The EM force field presents a complex spatial distribution, and the curl of EM forces acts as an additional source of vorticity as shown in the Navier-Stokes and vorticity equations:

$$\rho\frac{d\mathbf{U}}{dt}+\nabla P+\rho\,\mathbf{g}=\mu\,\nabla^2\mathbf{U}+\mathbf{j}\times\mathbf{B} \qquad (1)$$

$$\rho\frac{d\boldsymbol{\omega}}{dt}=\rho\,\boldsymbol{\omega}\cdot\nabla\mathbf{U}+\mu\,\nabla^2\boldsymbol{\omega}+\nabla\times(\mathbf{j}\times\mathbf{B}) \qquad (2)$$

It is remarkable that the source terms, appearing at the right hand side of equations (1) and (2), are quasi-independent of the velocity field. This is mostly due to the poor apparent electrical conductivity of seawater.

Most of the published experimental studies concern EMFC of turbulent boundary layer (Nosenchuck & Brown 1993, Henoch & Stace 1995). In such a complex situation it is difficult to outline the dominant mechanisms. Nevertheless, Acarlar & Smith (1987) have shown the possibility to produce a kind of « synthetic turbulent boundary layer », that is in fact an hairpin vortex street produced by a hemispheric protuberance, easily identifiable and reproducible. This kind of boundary layer presents a great analytic interest, since the hairpin vortices are associated with the generation and transport of turbulent energy (Robinson, 1991).

The first part of this work presents an experimental investigation of the influence of a normal electromagnetic actuator on a hairpin vortex street generated by a hemispherical wall protuberance. The objective is to identify and understand the mechanisms involved in the EMFC of hairpin coherent structures.

The second part of this work presents a numerical study aiming at a better understanding on the mechanisms involved in EMFC. The first numerical approach consists of the study of an unsteady laminar case using a finite volume code. A comparison to previous experimental results is then possible. The flow is well estimated except in the region close to the wall. The second numerical approach focuses on the wall region of a turbulent boundary layer. For that a direct

numerical simulation (DNS) based on Paulo Orlandi's code is undertaken (Orlandi, 2000). The steps of the procedure are the following. An ordinary turbulent boundary layer is computed and the coherent structures in this boundary layer are identified. Then various local forcing of these structures (source of force and source of vorticity) are performed and the response of the flow is analysed.

EXPERIMENTS

Experimental Setup

The experiments have been conducted in a close circuit water tunnel, illustrated in the Figure 2. The test section, measuring 100 × 100 × 1700 mm and capable of flow speeds up to 2 m/s, is entirely made of Plexiglas.

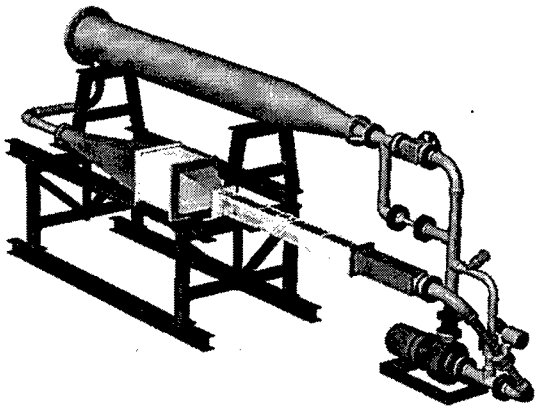

Figure 2 : Closed circuit water tunnel.

The working fluid (35 g/l NaCl aqueous solution) corresponds to standard seawater having an electrical conductivity of about 5 S/m. Electrical power is supplied to the electrodes by an adjustable direct current generator. The EM actuator is mounted in the test section, 220 mm downstream the hemisphere having a radius R = 10 mm, as illustrated in the Figure 3. Thus the actuator is placed 22 R downstream the hemisphere in a square channel having a 10 R × 10 R cross section. The blockage ratio of the test section due to the hemisphere is of 1.6 %.

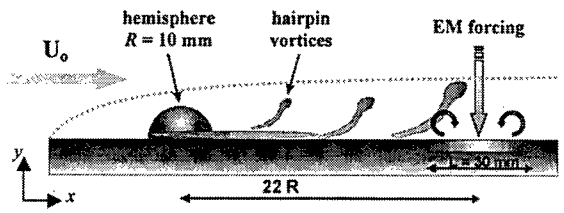

Figure 3 : Experimental setup in the water tunnel test section: hairpin vortex street shed by an hemispheric protuberance and EM forcing downstream.

In the median plan (normal to the wall), the flow may be considered as a flat plate boundary layer because the settling chamber upstream the test section re-initialises the incoming flow. PIV measurements give two-component velocity field at various positions (i.e. downstream the hemisphere and above the EM actuator). The frequency of the PIV measurements is 15 Hz.

Experimental Results

In order to characterise the hairpin vortex street shed by the hemisphere (without EM forcing), the shedding frequency has been measured for flow speeds in the range of 4 to 15 cm/s. The Reynolds and Strouhal numbers are defined as

$$Re_R = \frac{U_o R}{\nu} \quad \text{and} \quad S = \frac{f R}{U_o} \qquad (3)$$

where U_o is the free flow velocity, R the hemisphere radius, ν the fluid kinematical viscosity and f the hairpin vortex shedding frequency. The obtained results are presented in the Figure 4 and compared with those of Acarlar & Smith (1987), showing good agreement.

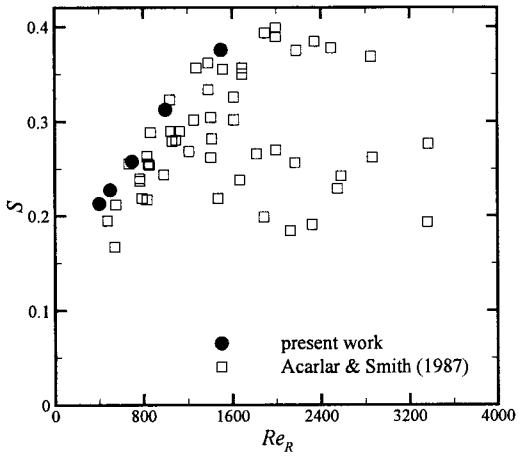

Figure 4 : Strouhal versus Reynolds number for a hemisphere (R = 10 mm).

Figure 5 shows an example of the flow field obtained by PIV measurements, where we can see the hairpin vortex street produced downstream a hemisphere (Re_R = 400). At the level of the hairpin "heads", the boundary layer downstream x/R = 4-5 presents regular spaced vorticity spots (Figure 5b). Note that the coordinate x is centred with the hemisphere, and V is the local velocity length $V = \sqrt{u^2+v^2}$.

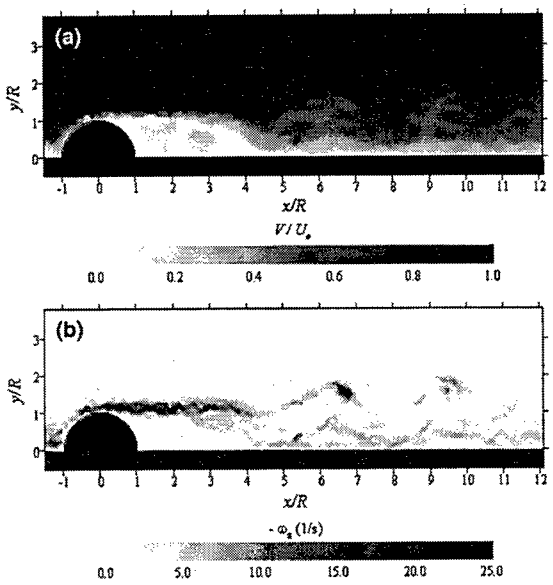

Figure 5 : PIV measurements downstream a hemisphere without EM forcing (Re_R = 400) : (a) velocity field; (b) vorticity field

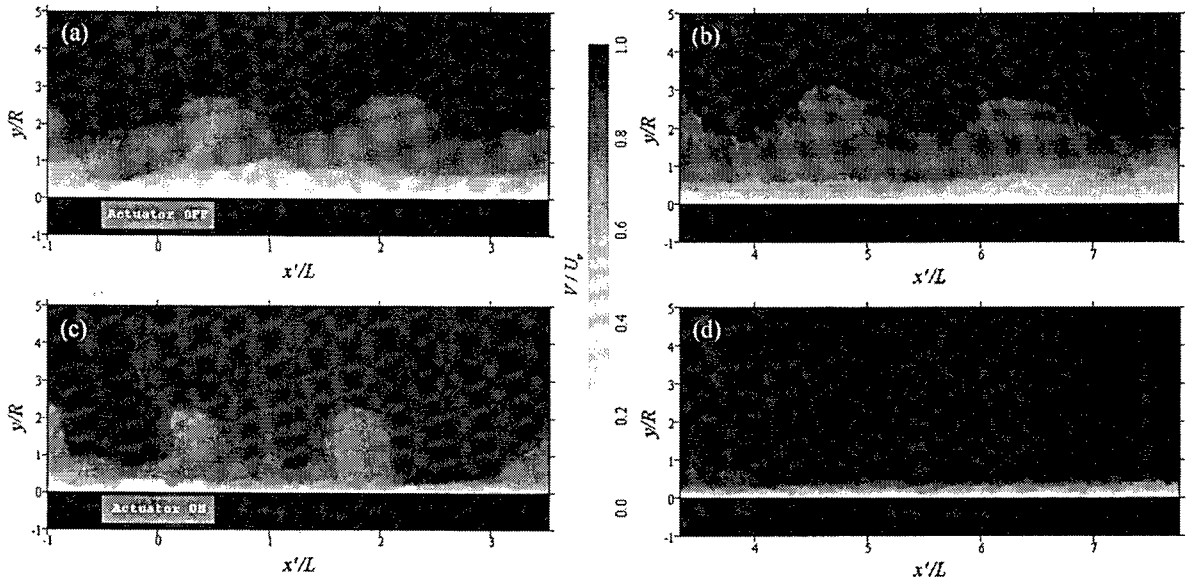

Figure 6: Hairpin vortex street generated by a hemisphere $22R$ upstream an EM actuator, velocity field obtained by PIV measurements ($Re_R = 500$): (a, b) without EM forcing; (c, d) with EM forcing (I=1A).

In order to investigate the EM forcing effect on the hairpin vortex street, the EM actuator placed $22\,R$ downstream the hemisphere is powered with a constant current of intensity I = 1 A.

Figure 6 shows flow fields over and downstream the EM actuator, with and without EM forcing (note that the coordinate x' is centred with the EM actuator, and V is the velocity length). Comparing Figures (a, b) and (c, d), one can see that the EM forcing can rapidly degenerate the hairpin vortex street downstream the EM actuator, which is completely eliminated from $x'/L = 4$.

This experiment demonstrates the possible very rapid destruction of the coherent motion of an hairpin structure. This is well explainable by the combined effect of 1) the stabilizing effect of the wall-normal downward flow induced by the EM forcing and 2) the cutting effect of diagonal wall jets observed in previous experiments (Rossi & Thibault 2002).

NUMERICAL SIMULATIONS

The final objective of numerical simulation of EMFC is very ambitious for two reasons: the difficulty of a turbulent wall bounded flow and the very complex 3D shape of the EM forces distribution. This last point is well established from previous experiments on the flow generated by an EM actuator from a flow initially at rest. Hopefully, due to symmetries in the forcing terms, the flow induced presents also symmetry plans especially for a flow initially at rest (Rossi 2001). Consequently two complementary approach of the entire problem are given here. i) a 2D simulation of the flow driven (starting from rest) by an EM actuation as close as possible of the real force distribution of the experiments. ii) a DNS of a turbulent wall bounded flow submitted to various forcing protocol.

Unsteady 2D laminar case

This first numerical 2D simulation takes place in the symmetry plan above the EM actuator. It consists to study the problem of an EM activation (starting from a flow at rest) in a 2D unsteady laminar case by using a finite volume code. Concerning the EM forces field which is strongly non-uniform but steady (Rossi 2001), we decided to model it, step by step, from a simplifying "bloc" distribution to progressively multi-bloc distribution closer from the real forcing term.

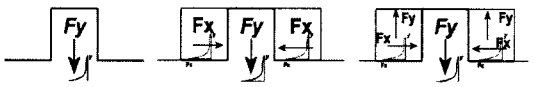

Case 1 Case 2 Case 3

Figure 7: Schematic of the step by step EM forcing model. In the 3 cases the forcing term is exponentially decreasing from a maximum at the wall (y = 0)

The comparison of previous experiments (see Figure 8) and present numerical results (see Figure 9) clearly shows a close similarity, except in the zone very close to the actuator. This is well explained regarding that wall diagonal jets are observed in the experiment. In fact these jets are flowing outward the simulation plan in the four semi-angle directions associated to the corner of the actuator angle (see figure 1). Thus nearby the wall the 2D simulation is not relevant. In other word a symmetry plan of the flow does not mean that the 2D divergence remains zero in any part of the flow domain.

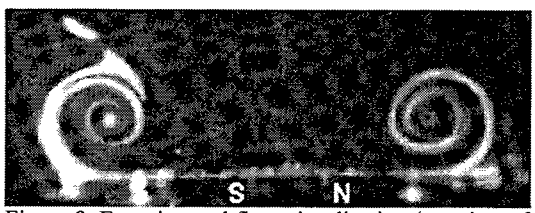

Figure 8: Experimental flow visualisation (cut view of the vortical structures produced by EM forces in a flow originally at rest (Rossi 2001)

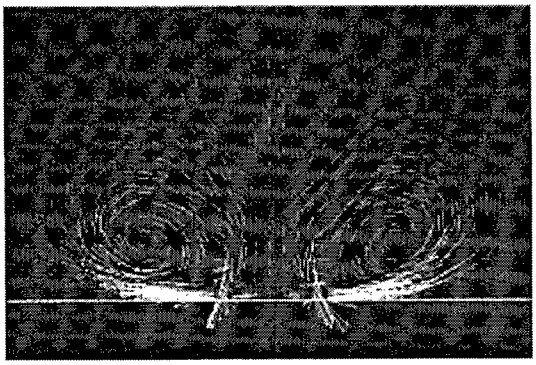

Figure 9: Computed flow produced by EM forces (case 2) in a flow originally at rest (Perrin 2001).

DNS approach

Simulation of an ordinary turbulent boundary layer (no forcing case). Our analysis is presently on progress and is using a DNS code (Orlandi 2000). The first step is to compute the ordinary turbulent boundary layer. The latter is going to be the initial condition preparing the next simulations with local injection (in space and time) of EM force source or EM vorticity source, finally premising to analyse the modified turbulent boundary layer.

The numerical solver uses finite differences schemes combine with a spectral method. Non-uniform meshes in the normal direction and periodic boundary conditions in the streamwise and spanwise directions are used. The necessary minimal mesh (256x129x128) is larger than that classically used for the simulation of unforced boundary layers. With a Reynolds number of 180 (in wall units) based on the wall shear velocity, the computational domain presented in figure 10 is ($4\pi h^+$, $4/3\pi h^+$ and $2h^+$) and the grid spacing is $\Delta x^+ \approx 8.8$ and $\Delta z^+ \approx 2.2$. The first mesh point, in the normal direction, is at $\Delta y^+ \approx 0.5$ from the wall and the maximum spacing is 5.6 wall units (at the center of the channel).

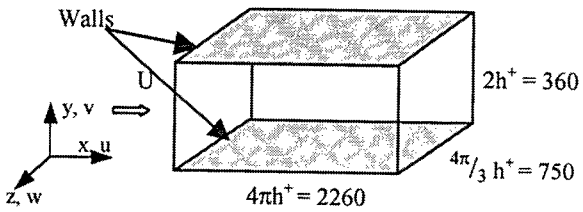

Boundary conditions: - Periodicity along x and z
- No-slip along y

Figure 10: Direct Numerical Simulation (DNS): Schematic of the computational domain and boundary conditions (box size in viscous wall units).

The first achievement is to obtain a fully turbulent flow starting from a laminar mean flow in which a small perturbation is imposed. Presently a fully turbulent solution is reached (from the statistical point of view) as shown on the figure 11. The present simulation is compared to those of Kim and al. (1987) which is classically taken as reference.

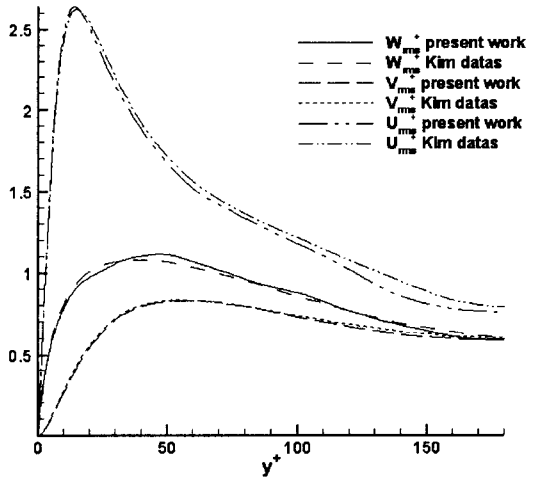

Figure 11: Velocity profile in viscous units: Comparison of the rms velocities between our simulation and the data of Kim et al. (1987).

Simulations of idealised modes of forcing (preliminary tests). Choi H. et al. (1994) showed that a forcing of the type "detection-action" allowed to reduce drag by about 25%. For that, the normal velocity fluctuations, detected at $y^+ = 10$, are numerically compensated directly by the creation at the wall ($y^+ = 0$) of a flow component equal and opposed to these fluctuations.

Table 1: Forcing type description

Type of forcing	Description
Choi	- detection of v' at $y^+ = 10$ - imposition of –v' at the wall
1	- detection of v' at $y^+ = 10$ - imposition of $f_y^+ = -1.8v'^+$ at $y^+ = 10$
2	- detection of v' at $y^+ = 10$ - imposition of $f_y^+ = -1.8v'^+$ from the wall to $y^+ = 10$
3	- application of a force $f_y^+ = -40$ in the volume ($y^+ = 0$ à 15).($x^+ = 0$ à 180).($z^+ =$ 120 à 160)
4	- actuator: at the wall, - size: 100^+ in x^+ and z^+. - EM forces for $\mathrm{Max}(f_{y\,EM}^+) = \mathrm{Max}(f_{y\,type\,2}^+)$

The mechanisms acting in this type of forcing (that one will call Choi's forcing) are compared, in our study, with other types of forcing. Using the same principle as Choi, but by applying a force proportional to the opposite of the normal velocity fluctuations and no longer to the wall but either at a given y^+ (forcing type 1) or from the wall to a given y^+ (forcing type 2), the effects on the flow differ radically (see the summary table at the end of the paragraph). Local forcing (forcing type 3) was also tested. The latter constitutes a first step towards the modelling of the real EM forcing (forcing type 4. Analytical solutions of the electric and magnetic fields are used to model EM forcing (Akoun & al., 1984). The EM force intensity used in DNS simulations is equivalent to that induced by forcing 2. It is almost 10^3 times less than the experimental one. Only its global and

not local effect is reported here. A spatial distribution of such MEMS actuators is currently investigated.

A significant drag reduction ($\tau^+ \equiv \partial u^+/\partial y^+$) at the wall (see figure 12) about 25%, by applying the Choi's forcing, is obtained, which is in agreement with the results of Choi for $t^+ = 1800$. This reduction is about 15% for the type 2 forcing, 1.5% for the type 1 forcing and around zero for the local forcing and real EM forcing. To sumarize it seems that acting only at the wall and on all surface is the most beneficial concept of forcing.

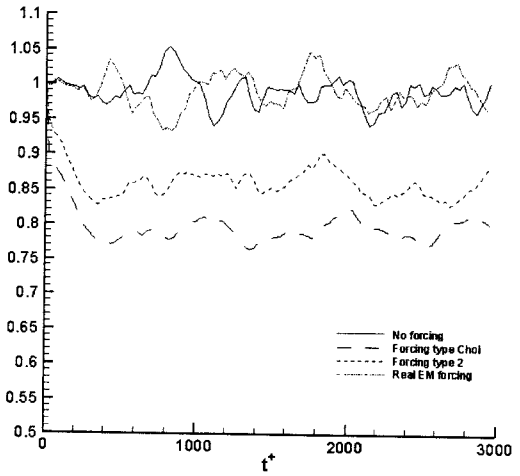

Figure 12: Comparison of the temporal evolution of the friction strain at the wall for different modes of forcing.

The layouts of the spanwise vorticity contours, for all types of forcing (see figures 13), show a decrease, in absolute value, of the intensities of this vorticity component. This remark is also true for the streamwise and normal components. Furthermore, the Choi's forcing seems to modify more actively the structures of the flow than the other forcings. In addition the EM forcing, although very local (the actuator (100^+ x 100^+) is located at the wall), which means that it acts on the structures of the flow eventhough it does not modify significantly the wall shear stress.

Table 2: Forcing action on structures

Type of forcing	**Reduction of τ^+**	**Action on the vorticity field** (criterium: global and not local)	
Choi	≈ 25 %	decrease of intensities	modification of structures
1	≈ 1.5 %	very small decrease of intensities	no modification of structures
2	≈ 15 %	small decrease of intensities	little modification of the structures
3	0 %	no decrease of intensities	no modification of structures
4	0 %	very small decrease of intensities	little modification of the structures

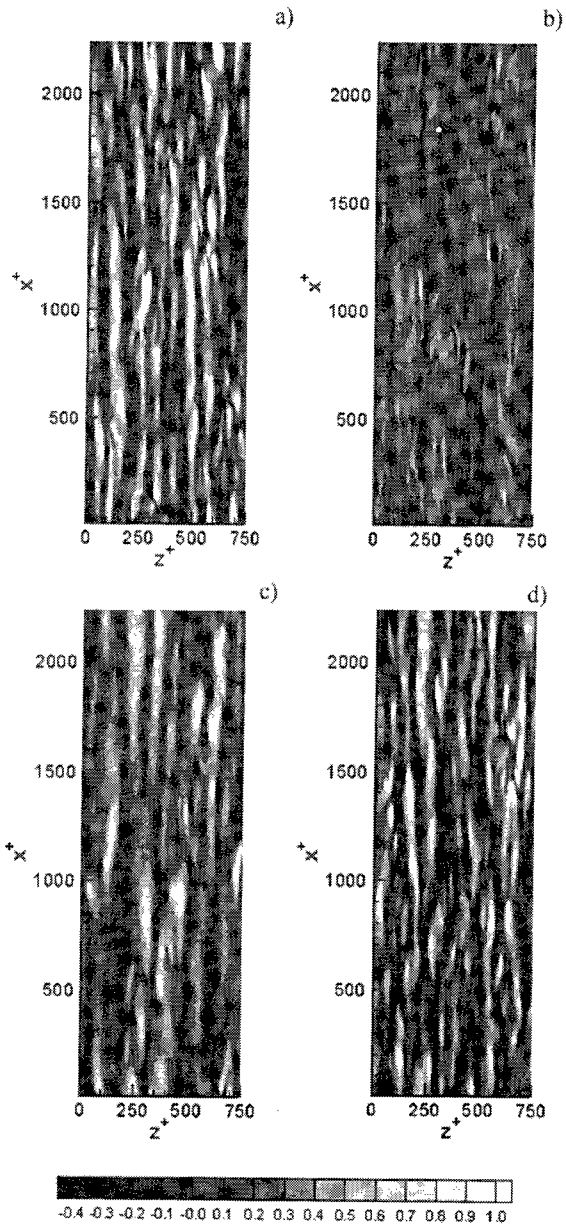

Figure 13 : Contours in viscous units: Spanwise vorticity at $y^+ = 4$ and $t^+ = 1800$.
a: No forcing,
b: Forcing type Choi,
c: Forcing type 2,
d: Forcing type 4.

The next step of this work on progress is the identification of coherent structures using for instance Q_2 (Willmarth *et al.*, 1972) and λ_2 (Jeong J. *et al.*, 1997) technic and then to apply local EM forces to these structures to get a better understanding of the process of disabling these structures by EM forcing.

SUMMARY AND CONCLUSIONS

EMFC is a novel concept that enables the direct injection of local body forces into the flow near the wall. This EM force field is also an important vorticity source, since its curl is not negligible.

The experimental investigation of the EM forcing of a hairpin vortex street produced by a hemisphere has shown its rapid degeneration downstream the EM actuator. This results give an experimental evidence that EMFC is a good candidate to control coherent motion in a turbulent boundary layer. For the future experimental tests, multiple actuators with pulsed forcing will be employed, as well as different actuator geometries.

The 2D finite volume numerical approach has shown its limits, even if the geometry and the flow present symmetry plans. The preliminary DNS calculations have enabled the validation of the code and the computational mesh, showing good agreement with Kim *et al.* (1987) data. A series of forcing protocols have confirmed the interest of the Choi's forcing type, even if its feasibility is not demonstrated. The first DNS calculations of an EM forcing have been accomplished with a geometry comparable to the experimental one (in wall units), but with a forcing intensity 10^3 times weaker. For the future, the EM forcing intensity will be progressively increased.

Both experimental and numerical approaches will be continued, aiming to identify the EMFC action modes on a turbulent boundary layer, and to optimise this concept to naval applications.

ACKNOWLEDGEMENT

This work was funded by DGA-DSP and DGA-BEC. Computations were done at the "Institut du Développement et des Ressources en Informatique Scientifique" (IDRIS). The second author also wish to thank CNPq-Brazil for the financial support.

REFERENCES

Acarlar M.S. & Smith C.R., 1987, "A study of hairpin vortices in a laminar boundary layer Part 1 : hairpin vortices generated by a hemisphere protuberance", *Journal of Fluid Mechanics*, vol.175, pp.1-41.

Akoun G. & Yonnet J-P., 1984, "3D analytical calculation of the forces exerted between two cuboidal magnets", *IEEE Transactions on magnetics*, vol. Mag. 20 n°5.

Bandyopadhyay R., 1998, "Drag reduction experiments on a small axisymetric body in saltwater using electromagnetic microtiles", *Proc. of the Int. Symp. on Seawater Drag Reduction*, Newport R. I., pp.457-461.

Choi H., Moin P. & Kim J., 1994, "Active turbulence control for drag reduction in wall-bounded flows", *J. Fluid Mech.*, 262, 75-110.

Jeong J. & Hussain F., 1997, "Coherent structures near the wall in a turbulent channel flow." *J. Fluid Mech.*, 332, 185-214.

Kim J., Moin P. & Moser R., 1987, "Turbulence statistics in fully developed channel flow at low Reynolds number", *J. Fluid Mech.*, vol.177, 133-166.

Henoch C. & Stace J., 1995, "Experimental Investigation of a Salt Water Turbulent Boundary Layer Modified by an Applied Streamwise Magnetohydrodynamic Body Force", *Phys. Fluids* 7 (6), pp.1371-1383.

Lim J., Choi H. & Kim J., 1998, "Control of streamwise vortices with uniform magnetic fluxes", *Phys. Fluids* 10(8).

Nosenchuck D.M, 1996, "Boundary layer control using the Lorentz force", *ASME Fluids Engineering Meeting*, San Diego.

Nosenchuck D.M. & Brown G.L., 1993, "The direct control of wall shear stress in a turbulent boundary layer", *Proc. of the Int. Conf. on Near Wall Turbulent Flows*, Princeton, Elsevier, pp.689-698.

Orlandi P., 2000, "Fluid Flow Phenomena, a Numerical Toolkit", Kluwer academic publishers, pp 3-51 and 188-230,.

Perrin M., 2001, "Contrôle électromagnétique de la turbulence: premiers pas en modélisation numérique", DEA Report, INPG, Grenoble, France.

Robinson S.K., 1991, "Coherent motions in the turbulent boundary layer", *Ann. Rev. Fluid. Mech.* 23, pp.601-39.

Rossi L., 2001, "Contrôle électromagnétique d'écoulements en eau de mer", Phd Thesis, Univ. Joseph Fourier, Grenoble, France.

Rossi L. & Thibault J-P., 2002, "Investigation of wall normal electromagnetic actuator for seawater flow control", *Journal of Turbulence* 3, 005.

Willmarth W. W. & Lu S. S., 1972, "Structure of the Reynolds stress near the wall.", *J. Fluid Mech.*, 55, 65-92.